Pixel-based trends mappings in the Guinea Region of West Africa: Integrating Remote Sensing Data and MODFLOW Modeling for Sustainable Resource Management and Monitoring

Abstract

Groundwater is vital in ensuring water security, supporting agriculture, and sustaining ecosystems in the Guinea region of West Africa. However, the region faces increasing challenges related to groundwater availability and quality due to population growth and climate change. This research presents pixel-based spatial-temporal trends assessment of groundwater mappings using an integrated approach that combines remote sensing data with MODFLOW modelling. The study focuses on the Guinea region, characterized by diverse topography and hydrogeological conditions. Remote sensing data, including satellite imagery of shallow groundwater storage (GWS), relative humidity, temperature, NDVI, and rainfall, provided valuable insights into observing hydrological cycles and climate changes. The MODFLOW modelling framework was employed to simulate groundwater flow (Hydraulic Heads) and variability of groundwater levels. It enabled the investigation of groundwater recharge and discharge processes, as well as the impact of climatic variations on groundwater dynamics.Furthermore, the trend modelling approach facilitated and revealed that the direction of the western to the northern part of the study area suffered from a depletion rate of groundwater level. The integrated analysis of remote sensing data and MODFLOW modelling highlights the complex interactions between climate change and groundwater resources. This research underscores the importance of proactive and informed groundwater management strategies to ensure the sustainable use of this invaluable resource. By combining remote sensing technology and groundwater modelling, it offers a holistic approach to support evidence-based decision-making for groundwater resource management and monitoring in the Guinea region of the West Africa**.**

Keywords- MODFLOW, NDVI, Shallow Ground Water Storage (GWS)

1. Introduction

Groundwater is a critical and invaluable resource that provides water security, sustains ecosystems, and supports agriculture in the diverse and dynamic Guinea region of West Africa (Bjornlund, V. et al. 2020). This vital resource underpins various human and ecological needs (Boltz F et al. 2019), highlighting the significance of its conservation and sustainable management. However, with its complex geography and hydrogeology, this region faces increasing challenges regarding groundwater availability, quality, and sustainability (Shah et al. R et al., 2020). Population growth and the ongoing effects of climate change have created uncertainty about the future of vital groundwater resources in this area (Seddon et al., 2020). The critical requirement for efficient groundwater management strategies necessitates inventive and data-led resolutions (Chuvieco, E, 2020). In response to this urgency, the research presented in this paper embarks on a journey to explore, assess, and analyze the state of groundwater resources in the Guinea region, leveraging cutting-edge methodologies that merge the power of remote sensing with the precision of MODFLOW modelling (Molina-Navarro, E, 2019). Our research focuses on unveiling the intricate dynamics of groundwater resources, which are vital for human consumption and critical for maintaining the equilibrium of the region's ecosystems. The Guinea region of West Africa encompasses a wide range of environmental and hydrogeological conditions, making it a particularly fascinating area for groundwater research (Ndehedehe et al., 2019). Groundwater in this region is integral to the lives of millions of people, providing a source of potable water, supporting the agricultural sector, and sustaining the area's rich biodiversity (Hiscock et al., 2011). The significance of groundwater in the Guinea region is deeply ingrained in the region's social, economic, and ecological fabric (Zabbey N et al., 2019). Population growth, urbanization, and the spectre of climate change pose formidable challenges to groundwater sustainability in this region (Planey, D. A. 2020). The demand for water resources, particularly from agricultural and industrial sectors, is rising (Hejazi, M, 2023). Simultaneously, altered precipitation patterns and increased temperatures, attributed to climate change, alter the region's hydrological dynamics (Stephens et al., 2021). In response to these challenges, this research adopts a holistic approach that combines remote sensing technology's analytical power with the MODFLOW groundwater modelling framework's predictive capability (Mengistu et al., 2019). This integrated approach enables a comprehensive understanding of groundwater trends, offering insights into the complex interactions between climate variability and groundwater resources.

The present research employs state-of-the-art remote sensing techniques to gather data on various environmental parameters. Satellite imagery is harnessed to monitor shallow groundwater storage (GWS), relative humidity, temperature, the Normalized Difference Vegetation Index (NDVI), and rainfall patterns. Integrating these datasets allows us to decipher the intricate hydrological cycles and explore the influence of climate variations on groundwater resources. In concert with the remote sensing data, we harness the robust MODFLOW modelling framework (Adams, K. et al., 2022). MODFLOW is an established tool that simulates groundwater flow and hydraulic head variations with high precision (Khadri R. et al., 2016). By employing this framework, we gain the capacity to delve deep into groundwater movement, recharge-discharge processes, and the intricate influence of climatic fluctuations on groundwater levels within the Guinea region (Serdeczny et al., 2017). The heart of this research lies in assessing trends in groundwater levels, with a particular focus on areas experiencing notable depletions. In the western to northern sectors of the study area, a pronounced depletion rate of groundwater levels has emerged, necessitating in-depth investigation and proactive management strategies. The core objective of this research is to highlight the complex and multifaceted interactions between climate change and groundwater resources in the Guinea region. The findings provide insights into the present state of groundwater resources and offer a glimpse into future challenges and opportunities.

Comment [g1]: Abbreviations are written in full in the beginning and in the rest of the text as abbreviations

1.Study area and its geology

Guinea, a country in West Africa with a total surface area of 278,519 square km, features a diverse geological landscape shaped by various geological processes over time(Kegler, S. R., & Butler, J. A. 2003).The study area, as illustrated in Figure 1, is characterized by the influence of Precambrian crystalline and Palaeozoic Rocks (Rollinson, H., 2016).The West African Craton, a stable geological entity, forms the fundamental geological framework for Guinea, providing a basis for understanding its geological diversity (Davison, I. 2005). The Man-Leo Shield, a crucial component of Guinea's basement geology, showcases Archean granite-gneiss complexes, offering insights into the region's Precambrian evolution (Lebrun, E. et al., 2017).In addition to the crystalline rocks, Guinea's geological story includes sedimentary basins like the Bove Basin (Machens, E. 1973).The Mesozoic-Cenozoic sedimentary infill within the Bove Basin holds significant potential for hydrocarbon exploration, contributing to the economic importance of the region (Dailly, P., 2000).The Fouta Djallon volcanic massif, a prominent geological feature, is

comprised of Neoproterozoic volcanic rocks, providing a window into the magmatic evolution of Guinea (Dailly, P., 2000).The intricate tectonic history of the region is revealed through fault systems and shear zones, adding another layer to Guinea's geological complexity (Dailly, P., 2000).The coastal zone introduces a geomorphological dimension influenced by both geological and climatic factors, showcasing the dynamic interaction between land and sea. The eastern part of Guinea is primarily underlain by Archaean and Lower Proterozoic rocks (Dailly, P., 2000)representing a significant geological foundation. In the north, upper Proterozoic metasedimentary rocks prevail, adding to the geological diversity of Guinea.The coastal plains, a distinctive feature of Guinea's geography, were predominantly formed by Quaternary marine and unconsolidated alluvial sediments (Dürr, H. H et al., 2005). This geomorphological characteristic is influenced by both geological and climatic factors, showcasing the dynamic interaction between land and sea.

2.1 Methodology (Trend Modeling)

The first modelling process used in this research was a pixel-based Mann-Kendall trend analysis (Fensholt et al., 2009, Neeti, N., & Eastman, J. R., 2009) on raster surfaces of remote sensing data (GWS, NDVI, relative humidity, temperature and precipitation). The Mann-Kendall test was applied to determine the statistical significance of the trend while Sen's slope estimator (Sobrino & Julien, 2013) was used to estimate the magnitudes of the trend. One advantage of this test is that it is not affected by missing data, while another benefit is that the data need not conform to any specific distribution (Jaagus, 2006). The null hypothesis for the Mann-Kendall nonparametric test is Ho, while the alternative hypothesis (H1) states that the distributions of xk and xj are not the same for all k and j $\leq$ n, where k $\neq$ j. The Mann-Kendall (M.K.) test statistic, denoted by S, has a mean of zero and the variance is estimated from equation (3).

$$S= \sum_{i=1}^{n-1} \sum_{j=i+1}^{n} \text{sgn}\,(xj - xk) \text{----------(1)}$$

Where xj and xk represent n data points at times j and k respectively, and sgn is the sign function defined by:

$$\text{sgn} = \begin{cases} 1 & \text{if } (xj - xi) > 0 \\ 0 & \text{if } (xj - xi) = 0 \\ -1 & \text{if } (xj - xi) < 0 \end{cases} \text{----------(2)}$$

For higher values of n, where n>= 10, the M.K. test statistics S follows the approximately normal distribution with mean as zero and variance V(s) as computed by equation (3):

$$V(s) = n(n-1)(2n+5) - \sum_{j=1}^{p} tj(tj-1)(2tj+5)/18 \text{ ---------(3)}$$

Where n refers to the number of data points, tj specifies the number of data points in the pth group. Tied groups (a tied group is a set of sample data having the same value) represented are by p. tj is the number of data points in the jth tied groups (Silva et al., 2015). The probability associated with S (equations 1 & 2) and the sample size n were statistically computed to quantify the significance of the trend. Then, the normalized test statistics Zmk computes using equation (4) as given below:

$$Z_{mk} = \begin{cases} \frac{S-1}{\sqrt{var\,(s)}}, & \text{when } s > 0 \\ 0, & \text{when } s = 0 \\ \frac{S-1}{\sqrt{var\,(s)}}, & \text{when } s < 0 \end{cases} \text{ ----------(4)}$$

The null hypothesis is rejected at a confidence level of 99% if the p-value is greater than or equal to 0.01. Similarly, if the p-value is greater than or equal to 0.05 at a confidence level of 95%, the null hypothesis is rejected. Equation 4 indicates that the resulting trend could be positive, negative, or zero (indicating no trend), with a corresponding level of confidence.

2.2 Methodology (MODFLOW modelling)

The second part of the modelling work was to perform MODFLOW modelling for heads (Groundwater level), which included various conceptual and numerical techniques (Chiang, W. H., &Kinzelbach, W. 1998).The hydrogeological study of the Guinea region in West Africa involves multifaceted MODFLOW modeling for groundwater levels. Utilizing various conceptual and numerical techniques, MODFLOW is the international standard for predicting groundwater conditions and interactions with surface water. The methodology includes gathering field data incorporating topographical elevations from the Digital Elevation Model (DEM), river water levels, and hydrological features. Rainfall data indicates an annual average of 2049 mm,

with initial hydraulic heads ranging in different blocks. The 3D aquifer model integrates DEM and aquifer depth. Model calibration checks reliability under natural conditions, and steady-state flow simulations consider the variable hydraulic head boundary conditions. The water budget serves as an overall acceptability indicator for the numerical solution, emphasizing continuity in total flows. The study's comprehensive workflow involves constructing the aquifer body model, model calibration, and assessing the impact of river systems on groundwater dynamics.A step-by-step methodology is shown in the following workflow diagram in Figure 2.

3. Results and Discussions

The primary focus of this study is the Shallow Groundwater Storage (GWS) modelled in the Catchment Land Surface Model (CLSM) as part of the Global Land Data Assimilation System (GLDAS). Specifically, GWS denotes the water below the soil layer's root zone and above the bedrock. The formula used to isolate GWS from the other water storage variables in the CLSM is as follows: shallow groundwater storage (GWS) can be calculated by subtracting root zone soil moisture, snow water equivalent, and canopy interception from total water storage (TWS). Based on the monthly (Jan-Dec) spatial distribution of GWS for 2022 (Figure 4d), it was observed that the central to southern region of Guinea exhibited the highest groundwater storage (Figure 4d). This area predominantly encompasses Mamov, Babola, Faramah, Kanan, Sako, Sopota, and Nzerekare. Groundwater storage in this region ranges from 1000mm to 2000mm. Additionally, the observed minimum of groundwater storage is located in the Western-Northern-Eastern direction, as shown in Figure 4d. Notably, the monthly spatial distribution of rainfall maps in Figure 4a highlights that rainfall is highest in the western to northern periphery of the study area. Conversely, the minimum groundwater storage is found in the same region where maximum rainfall is observed, as illustrated in Figure 4a. The spatial distribution analysis of temperature variables (Figure 4b) in the study region reveals that the highest temperature is observed towards the west-north-east direction, which also records the maximum rainfall (Figure 4a). Figure 4c shows that the highest relative humidity (%) is observed in August, July, June, and September. The present research work is statistically modelled in the box plots shown in Figure 3. The statistical analysis of monthly groundwater storage (GWS) for the Guinea region in West Africa showed that maximum and minimum GWS occurred in October and January, respectively, in the year 2022, as illustrated in Figure 3. Similarly, the respective maximum and minimum rainfall for the same region, shown in Figure 4a, were recorded during January and June. The findings

show that the highest amount of rainfall (Figure 4a) occurs in June (6), which is the monsoon season in the Guinea region, while the maximum amount of Groundwater Storage (GWS) is observed during October (10), which is the post-monsoon season within the study area of Guinea, West Africa. These results suggest groundwater recharge via infiltration is taking place, which is a favourable signal for the study region. The temperature, relative humidity, and rainfall of box plots indicate the specific months when the temperature (Figure 3) was at its lowest and the relative humidity and rainfall were at their highest (Figure 3). MODFLOW is widely recognized as the international standard for predicting and modelling groundwater conditions and interactions between groundwater and surface water (M. et al. et al., 2012). Guinea is the origin of more than 20 rivers in Western Africa. The Fouta Djallon is the source of the region's three main rivers. The Niger River and its several tributaries, such as the Tinkisso, Milo, and Sankaran, have their sources in the highlands, flowing in a northeasterly direction across Upper Guinea to Mali. The water level of this river provides constantly changing head boundary conditions. The groundwater model encompasses an area of 278,519 square kilometres, with each model grid cell measuring 5x5 square kilometres. Figure 6a &6b illustrates the cross-section of the model's subsurface formation and hydraulic heads (groundwater level) in 3D. To evaluate the model's performance, calibrated water levels were compared with observed groundwater levels, revealing similarities in groundwater table fluctuations near rivers and seasonal river level fluctuations. Budget Calculation (Cubic metres) computes the budget of user-specified zones and the exchange of flows between them (Table 1). A water budget serves as an indicator of the numerical solution's overall acceptability. In numerical solution techniques, the solved equations system of a model includes a flow continuity statement for each model cell. It is essential for continuity to exist in the total flows into and out of either the entire model or a sub-region. This indicates a steady-state flow simulation where the total inflow and outflow should balance at zero.The horizontal hydraulic energy of the first and second stratigraphic units is 0.0001 m/s and 0.0005 m/s, respectively, and can be considered negligible. The vertical hydraulic heads, or groundwater levels relative to MSL, range between 10 and 120 meters (Figure 6b). The elevation of the ground surface, namely the top of the first stratigraphic unit or DEM, ranges from 7 to 800 meters (as seen in Figure 6a). The depth of the aquifer varies from 0 to 260 meters (Figure 6a). In order to assess the validity of the simulation results, MODFLOW calculates a volumetric water budget of heads (in cubic meters) for the entire model at the end of each time step between 2000 and 2022. This data is presented in Table 1. The water budget

serves as an indication of the general acceptability of the numerical solution. In numerical solution methods, the model's system of equations comprises a flow continuity declaration for every model cell. Continuity must also apply to the overall flows in and out of the whole model or a specific sub-region. Therefore, the total inflow minus the total outflow should equal 0 (steady-state flow simulation) or the total change in storage (transient flow simulation) while avoiding subjective evaluations unless clearly labelled. It was determined from the monthly time trend of GWS reduced between 23.5 mm/month to 10 mm/month from January to December 2022, under the direction of the western-central-northern region, as depicted in Figure 5a. It has been discovered through time trend modelling of the Normalized Vegetation Index (NDVI) for March 2010 to 2022 that vegetation has decreased towards the west-northern side (Figure 5d). Additionally, trend maps identified the maximum trend in relative humidity in the central-northern area (Figure 5b). Similarly, the monthly trend map of rainfall indicates a maximum observation in the western-eastern direction with a range of 41.65mm/month to 22mm/month (Figure 5d). The monthly trend maps of temperature (Figure 5c) for the year 2022, from January to December, show a decrease in temperature at a rate of 0.18 deg C/month to 0.05 deg C/month in the western region of the study area and an increasing trend was observed towards the eastern area with a rate of 0.02 to 0.08 deg C/month.

Comment [g2]: In this section, the findings need to be compared with the results of previous studies in this field

4.Conclusions

The current study is centered around five key meteorological variables: Groundwater Storage (GWS), rainfall, NDVI, temperature, and relative humidity. Observations based on rainfall data suggest that the infiltration process in the Guinea region is significantly lower in the western to northern direction when compared to the southern direction. This is primarily due to the fact that GWS values are notably lower in these regions compared to other parts of the study area. Another contributing factor to the reduced GWS in this region is the area's topographical characteristics. 3D and 2D Digital Elevation Model (DEM) visualizations of the study area indicate that GWS is at its minimum in higher elevation areas and maximum in lower elevation areas. Furthermore, the mudflow modeling, both conceptual and numerical, has revealed that groundwater heads, measured with respect to Mean Sea Level, vary within the range of 7 meters to 90 meters.Considering the holistic modeling, it is strongly recommended that increased attention should be directed towards the western and northern regions for the sustainable

development of groundwater levels. Failure to address the groundwater management system in this region could result in severe damage to both the surface and subsurface aquifer systems.

References

Bjornlund, V., Bjornlund, H., & Van Rooyen, A. F. (2020). Why agricultural production in sub-Saharan Africa remains low compared to the rest of the world–a historical perspective. *International Journal of Water Resources Development*, *36*(sup1), S20-S53.

Boltz, F., Poff, N. L., Folke, C., Kete, N., Brown, C. M., Freeman, S. S. G., ... &Rockström, J. (2019). Water is a master variable: Solving for resilience in the modern era. *Water Security*, *8*, 100048.

Shah, M. A. R., Renaud, F. G., Anderson, C. C., Wild, A., Domeneghetti, A., Polderman, A., ... & Zixuan, W. (2020). A review of hydro-meteorological hazard, vulnerability, and risk assessment frameworks and indicators in the context of nature-based solutions. *International journal of disaster risk reduction*, *50*, 101728.

Seddon, N., Chausson, A., Berry, P., Girardin, C. A., Smith, A., & Turner, B. (2020). Understanding the value and limits of nature-based solutions to climate change and other global challenges. *Philosophical Transactions of the Royal Society B*, *375*(1794), 20190120.

Chuvieco, E. (2020). *Fundamentals of satellite remote sensing: An environmental approach*. CRC press.

Molina-Navarro, E., Bailey, R. T., Andersen, H. E., Thodsen, H., Nielsen, A., Park, S., ... & Trolle, D. (2019). Comparison of abstraction scenarios simulated by SWAT and SWAT-MODFLOW. *Hydrological Sciences Journal*, *64*(4), 434-454.

Ndehedehe, C. E. (2019). The water resources of tropical West Africa: problems, progress, and prospects. *ActaGeophysica*, *67*(2), 621-649.

Hiscock, K. M. (2011). Groundwater in the 21st century–meeting the challenges. *Sustaining Groundwater Resources: A Critical Element in the Global Water Crisis*, 207-225.

Zabbey, N., Giadom, F. D., & Babatunde, B. B. (2019). Nigerian coastal environments. In *World Seas: an Environmental Evaluation* (pp. 835-854). Academic Press.

Planey, D. A. (2020). *Growth, prosperity, and inequality after the great recession: A regionalist cultural political economy of Chicagoland* (Doctoral dissertation).

Hejazi, M., Santos Da Silva, S. R., Miralles-Wilhelm, F., Kim, S., Kyle, P., Liu, Y., ... & Clarke, L. (2023). Impacts of water scarcity on agricultural production and electricity generation in the Middle East and North Africa. *Frontiers in Environmental Science*, *11*, 157.

Stephens, C. M., Lall, U., Johnson, F. M., & Marshall, L. A. (2021). Landscape changes and their hydrologic effects: Interactions and feedbacks across scales. *Earth-Science Reviews*, *212*, 103466.

Mengistu, H. A., Demlie, M. B., Abiye, T. A., Xu, Y., &Kanyerere, T. (2019). Conceptual hydrogeological and numerical groundwater flow modelling around the Moab Khutsong deep gold mine, South Africa. *Groundwater for Sustainable Development*, *9*, 100266.

Adams, K. H., Reager, J. T., Rosen, P., Wiese, D. N., Farr, T. G., Rao, S., ... & Rodell, M. (2022). Remote sensing of groundwater: current capabilities and future directions. *Water Resources Research*, *58*(10), e2022WR032219.

Khadri, S. F. R., & Pande, C. (2016). Ground water flow modeling for calibrating steady state using MODFLOW software: a case study of Mahesh River basin, India. *Modeling Earth Systems and Environment*, *2*, 1-17.

Serdeczny, O., Adams, S., Baarsch, F., Coumou, D., Robinson, A., Hare, W., ... & Reinhardt, J. (2017). Climate change impacts in Sub-Saharan Africa: from physical changes to their social repercussions. *Regional Environmental Change*, *17*, 1585-1600.

Kegler, S. R., & Butler, J. A. (2003). Traumatic Brain Injury-Related Hospital Discharges. *Morbidity and Mortality Weekly Report: MMWR. Surveillance Summaries. Surveillance summaries*, *52*.

Rollinson, H. (2016). Archaean crustal evolution in West Africa: A new synthesis of the Archaean geology in Sierra Leone, Liberia, Guinea and Ivory Coast. *Precambrian Research*, *281*, 1-12.

Davison, I. (2005). Central Atlantic margin basins of North West Africa: geology and hydrocarbon potential (Morocco to Guinea). *Journal of African Earth Sciences*, *43*(1-3), 254-274.

Lebrun, E., Miller, J., Thébaud, N., Ulrich, S., & McCuaig, T. C. (2017). Structural controls on an orogenic gold system: The world-class Siguiri gold district, Siguiri Basin, Guinea, West Africa. *Economic Geology*, *112*(1), 73-98.

Machens, E. (1973). The geologic history of the marginal basins along the north shore of the Gulf of Guinea. In *The South Atlantic* (pp. 351-390). Boston, MA: Springer US.

Dailly, P. (2000). Tectonic and stratigraphic development of the Rio Muni Basin, Equatorial Guinea: the role of transform zones in Atlantic Basin evolution. *GEOPHYSICAL MONOGRAPH-AMERICAN GEOPHYSICAL UNION*, *115*, 105-128.

Dürr, H. H., Meybeck, M., & Dürr, S. H. (2005). Lithologic composition of the Earth's continental surfaces derived from a new digital map emphasizing riverine material transfer. *Global Biogeochemical Cycles*, *19*(4).
Dürr, H. H., Meybeck, M., & Dürr, S. H. (2005). Lithologic composition of the Earth's continental surfaces derived from a new digital map emphasizing riverine material transfer. *Global Biogeochemical Cycles*, *19*(4).
Fensholt, R., Rasmussen, K., Nielsen, T. T., & Mbow, C. (2009a). Evaluation of earth observation based long term vegetation trends - Intercomparing NDVI time series trend analysis consistency of Sahel from AVHRR GIMMS, Terra MODIS and SPOT VGT data. *Remote Sensing of Environment*, *113*(9), 1886–1898. https://doi.org/10.1016/j.rse.2009.04.004

Fensholt, R., Rasmussen, K., Nielsen, T. T., & Mbow, C. (2009b). Evaluation of earth observation based long term vegetation trends - Intercomparing NDVI time series trend analysis consistency of Sahel from AVHRR GIMMS, Terra MODIS and SPOT VGT data. *Remote Sensing of Environment*, *113*(9), 1886–1898. https://doi.org/10.1016/j.rse.2009.04.004

Neeti, N., & Eastman, J. R. (2011). A Contextual Mann-Kendall Approach for the Assessment of Trend Significance in Image Time Series. *Transactions in GIS*, *15*(5), 599–611. https://doi.org/10.1111/j.1467-9671.2011.01280.x

Jaagus, J. (2006). Climatic changes in Estonia during the second half of the 20th century in relationship with changes in large-scale atmospheric circulation. *Theoretical and Applied Climatology*, *83*(1–4), 77–88. https://doi.org/10.1007/s00704-005-0161-0

da Silva, R. M., Santos, C. A. G., Moreira, M., Corte-Real, J., Silva, V. C. L., & Medeiros, I. C. (2015). Rainfall and river flow trends using Mann–Kendall and Sen's slope estimator statistical tests in the Cobres River basin. *Natural Hazards*, *77*(2), 1205–1221. https://doi.org/10.1007/s11069-015-1644-7

Chiang, W. H., &Kinzelbach, W. (1998). Processing modflow. *A simulation program for modelling groundwater flow and pollution. User manual.*

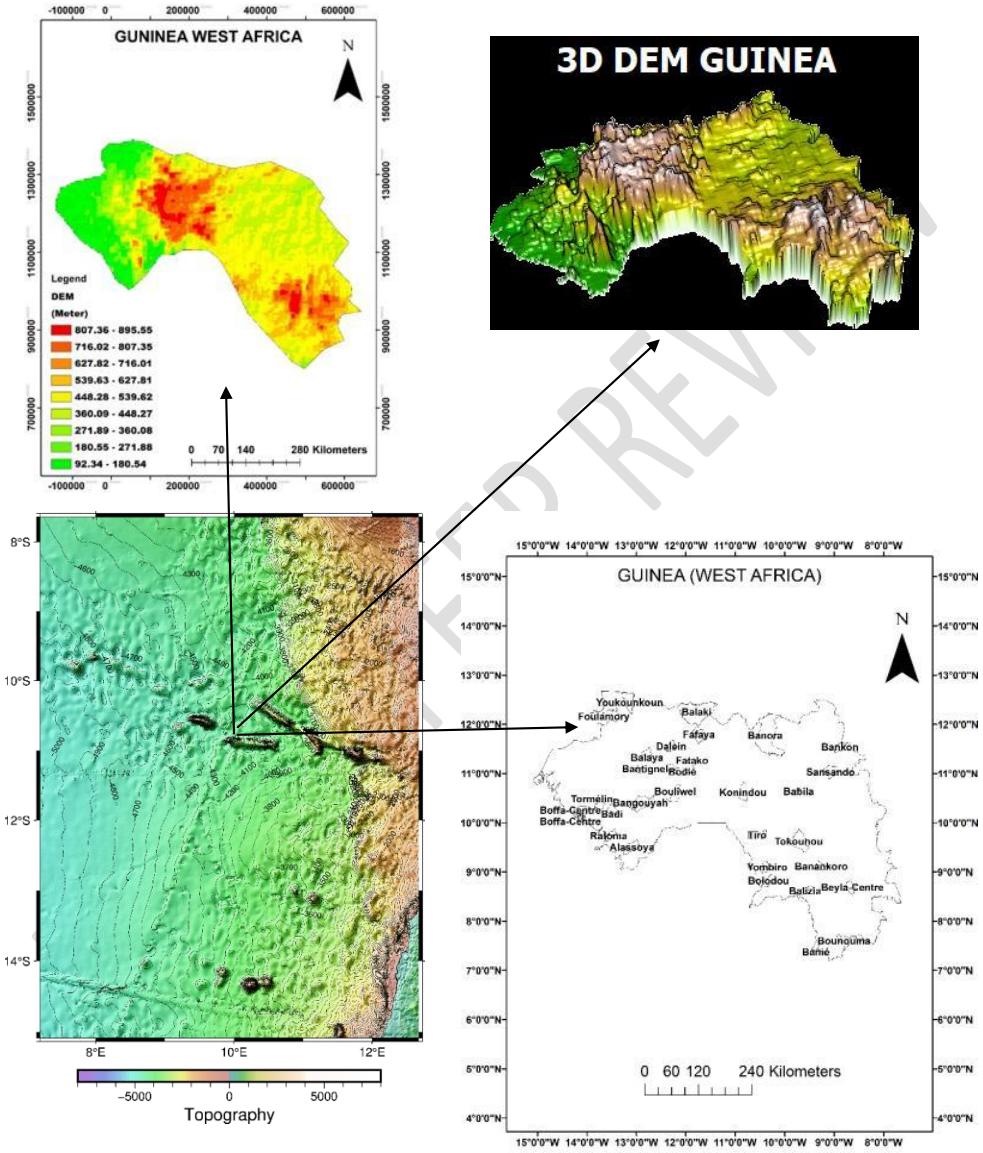

Figure 1 Study Area (DEM, Guinea, West Africa)

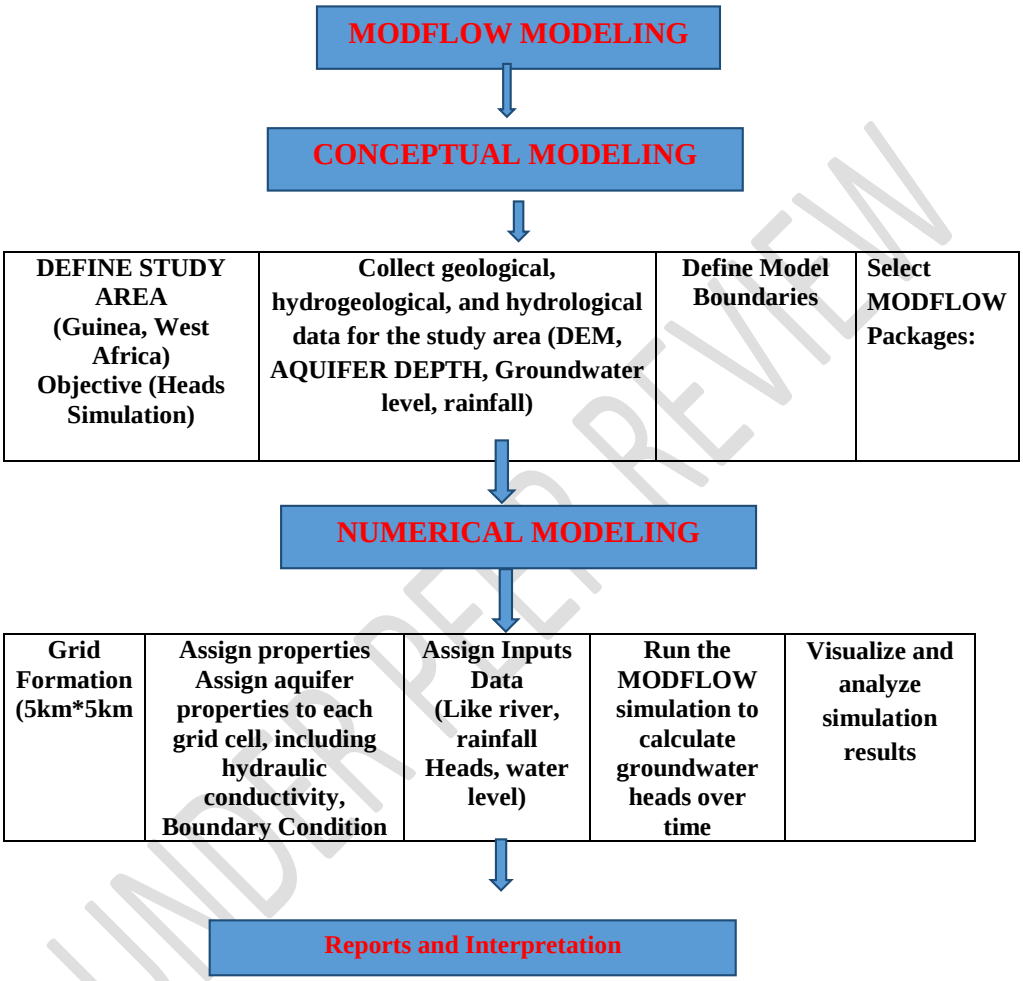

Figure 2 Work flow chart of MODFLOW processing

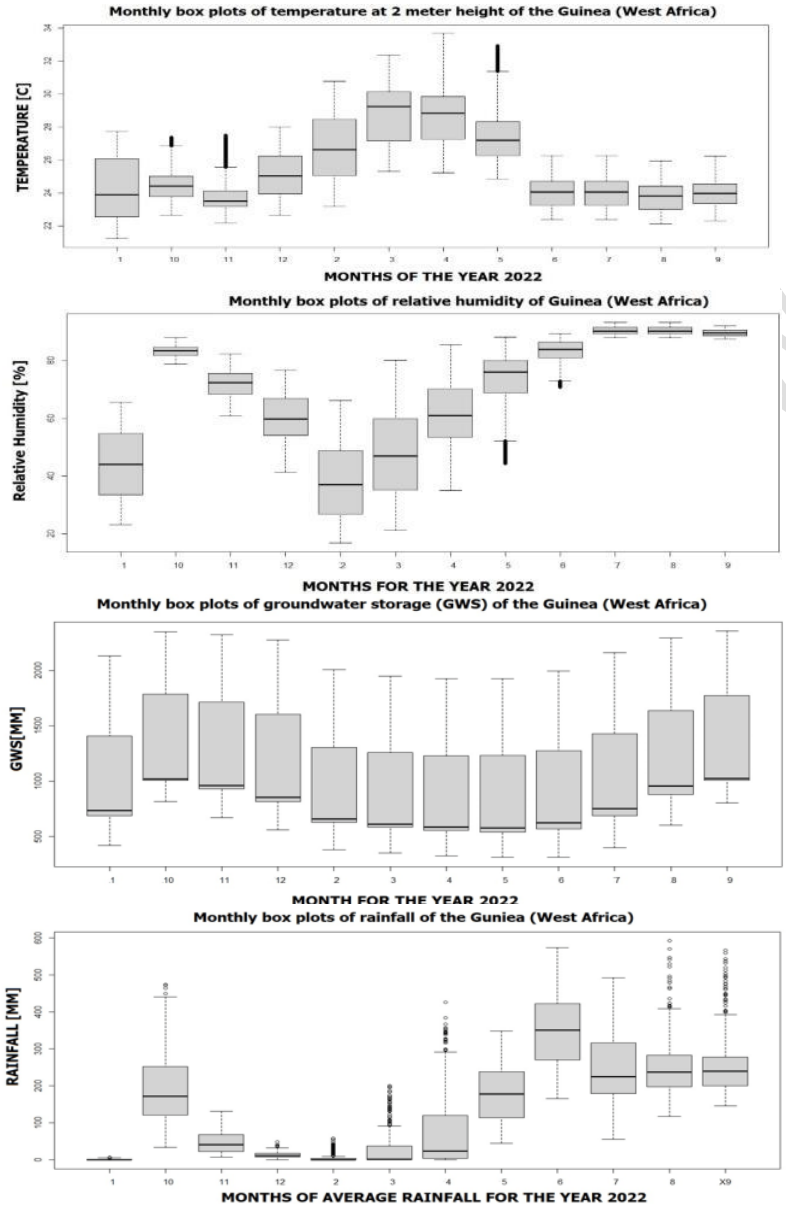

Figure 3 Box plots of monthly (Jan-Dec, 1-12) climatic valriables of temperature, raltive humidity, GWS and rainfall for the year 2022of Guinea (West Africa)

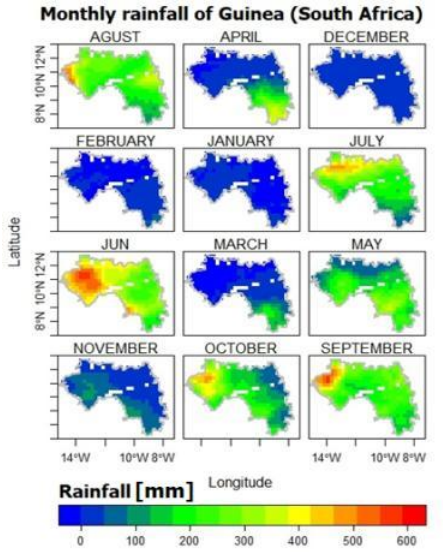

Figure 4 (a) Monthly spatial distribution of rainfall for the year 2022

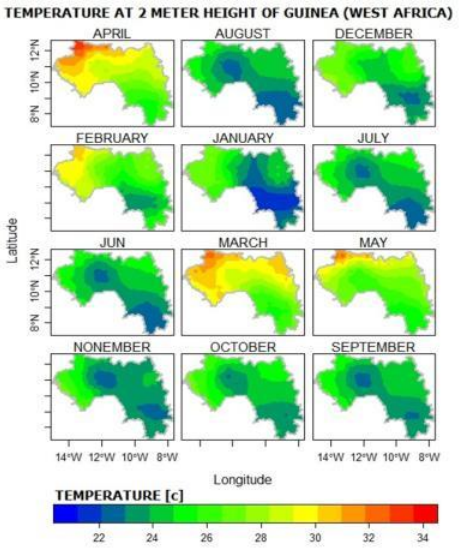

Figure 4 (b) Monthly spatial distribution of temperature at 2 m height for the year 2022

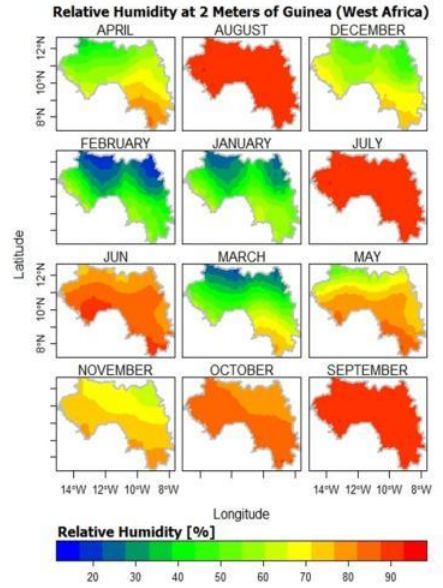

Figure 4 (c) Monthly spatial distribution of relative humidity for the year 2022

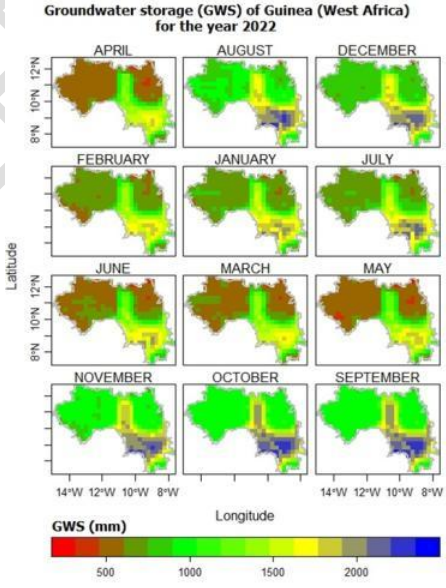

Figure 4 (d) Monthly spatial distribution of GWS for the year 2022

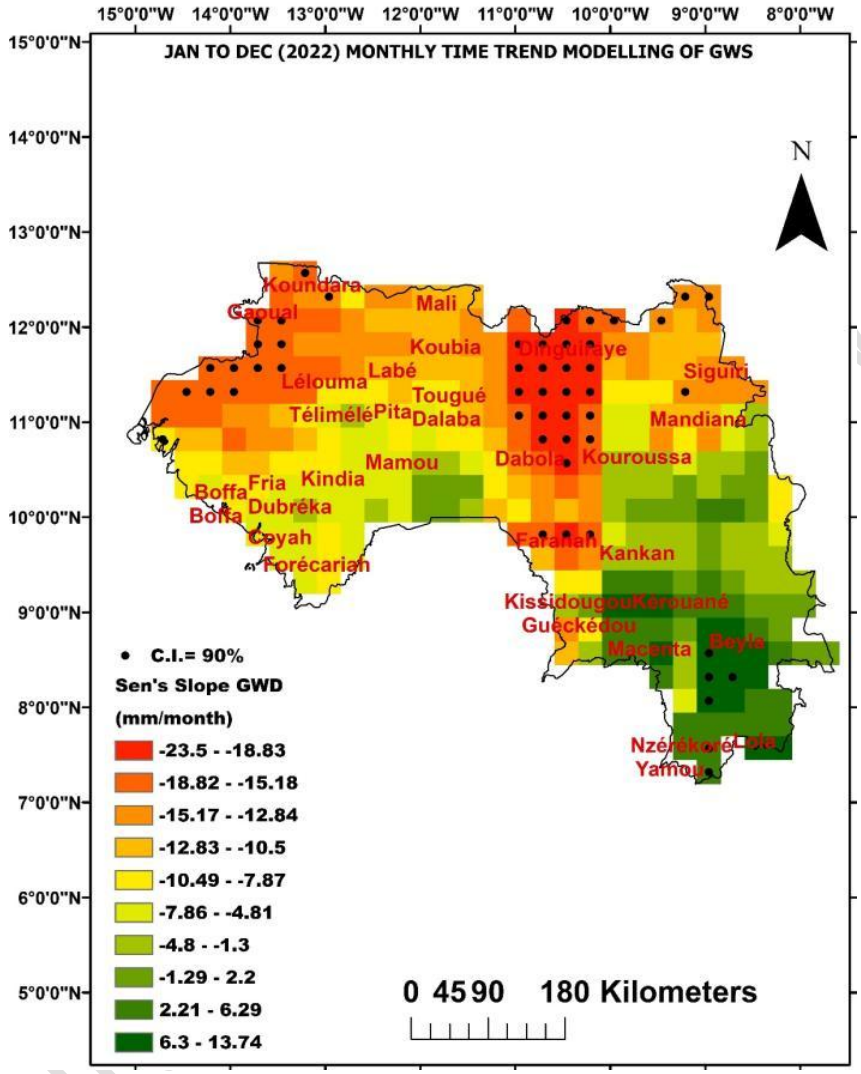

Figure 5 (a) Spatio-temporal monthly trend map of GWD for the year 2022

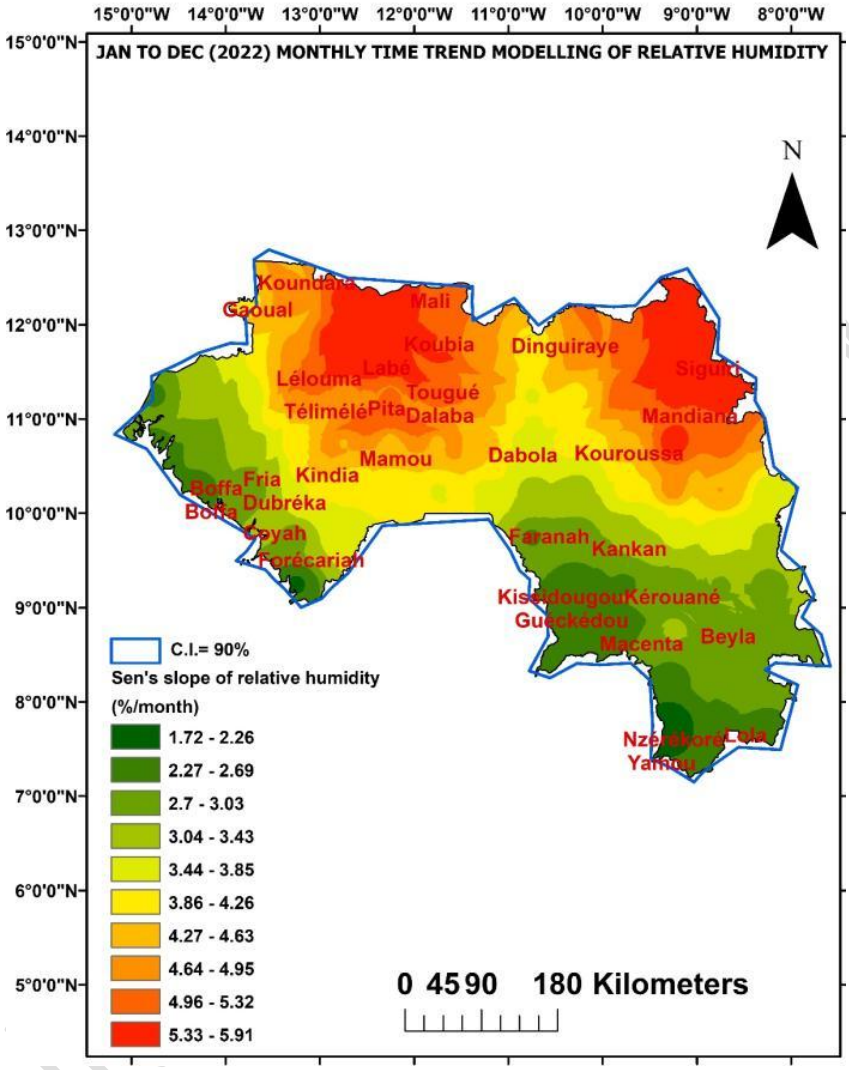

Figure 5 (b) Spatio-temporal monthly trend map of relative humidity for the year 2022

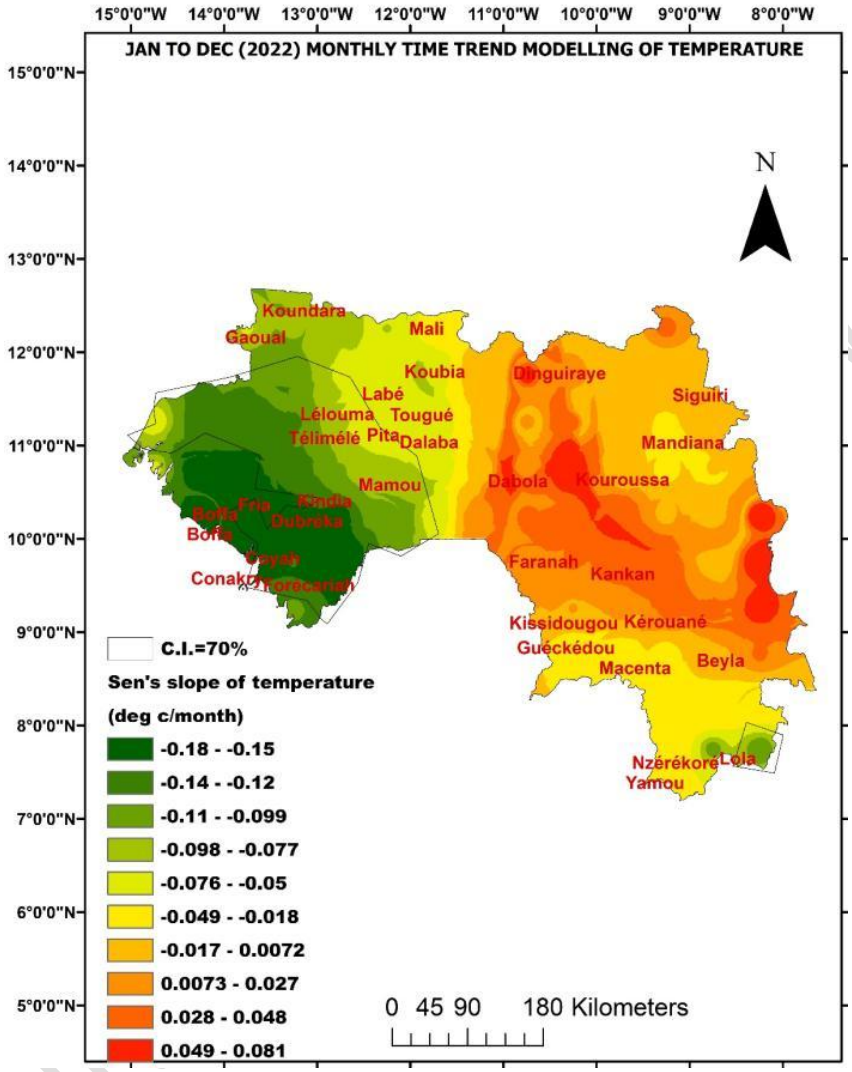

Figure 5 (c) Spatio-temporal monthly trend map of temperature for the year 2022

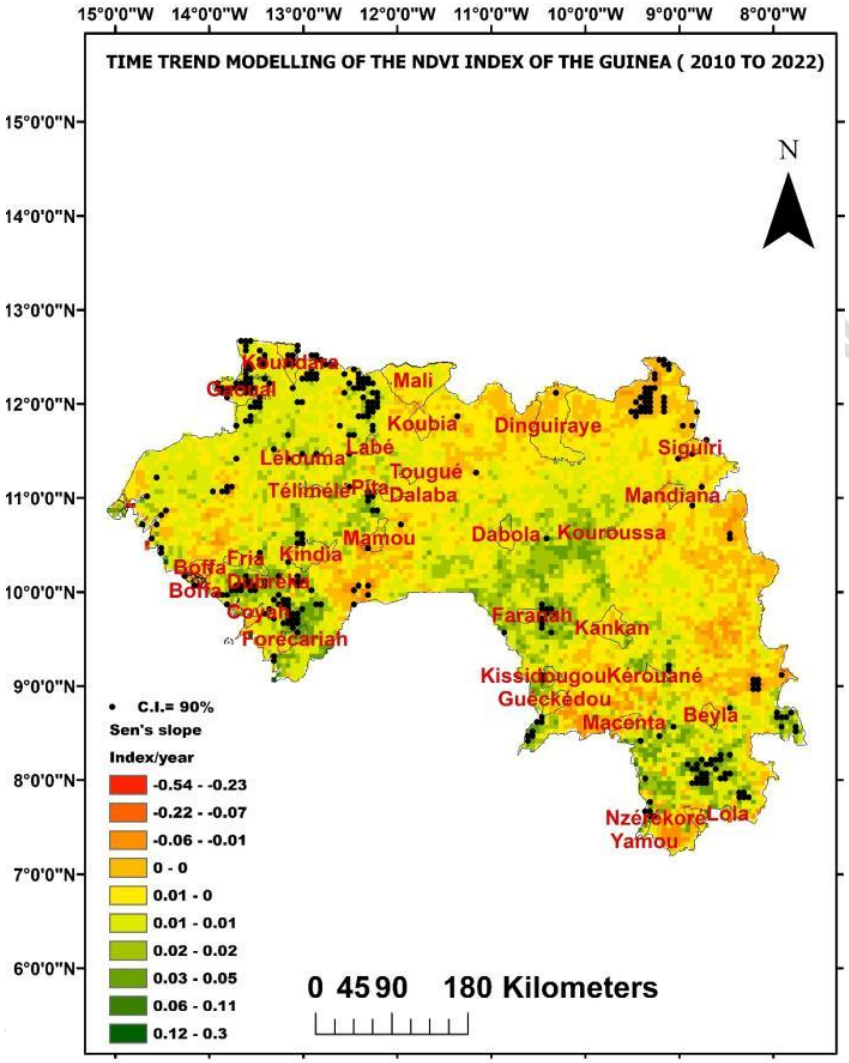

Figure 5 (d) Spatio-temporal trend map for the march month from the year 2010-2022 for the NDVI climatic variable

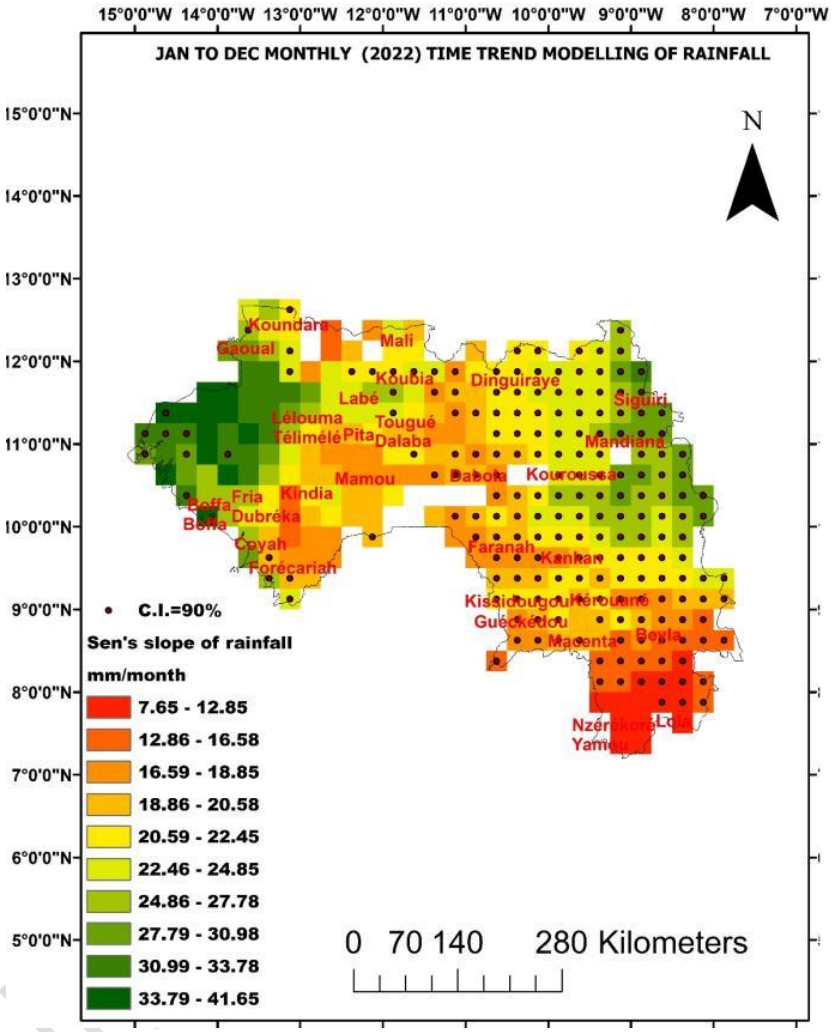

Figure 5 (d) Spatio-temporal monthly trend map of rainfall for the year 2022

Table 1: Volumetric budget for entire model at end of time step (Steady state) for groundwater level (Heads, Groundwater level)

VOLUMETRIC BUDGET FOR ENTIRE MODEL AT END OF TIME STEP 1 IN STRESS PERIOD 1

CUMULATIVE VOLUMES L**3		RATES FOR THIS TIME STEP L**3/T	
	IN:		IN:
	---		---
STORAGE =	0.0000	STORAGE =	0.0000
CONSTANT HEAD =	589820892.5515	CONSTANT HEAD =	589820892.5515
TOTAL IN =	589820892.5515	TOTAL IN =	589820892.5515
	OUT:		OUT:
	----		----
STORAGE =	0.0000	STORAGE =	0.0000
CONSTANT HEAD =	20645779.3085	CONSTANT HEAD =	20645779.3085
TOTAL OUT =	20645779.3085	TOTAL OUT =	20645779.3085
IN - OUT =	569175113.2430	IN - OUT =	569175113.2430
PERCENT DISCREPANCY =	186.47	PERCENT DISCREPANCY =	186.47

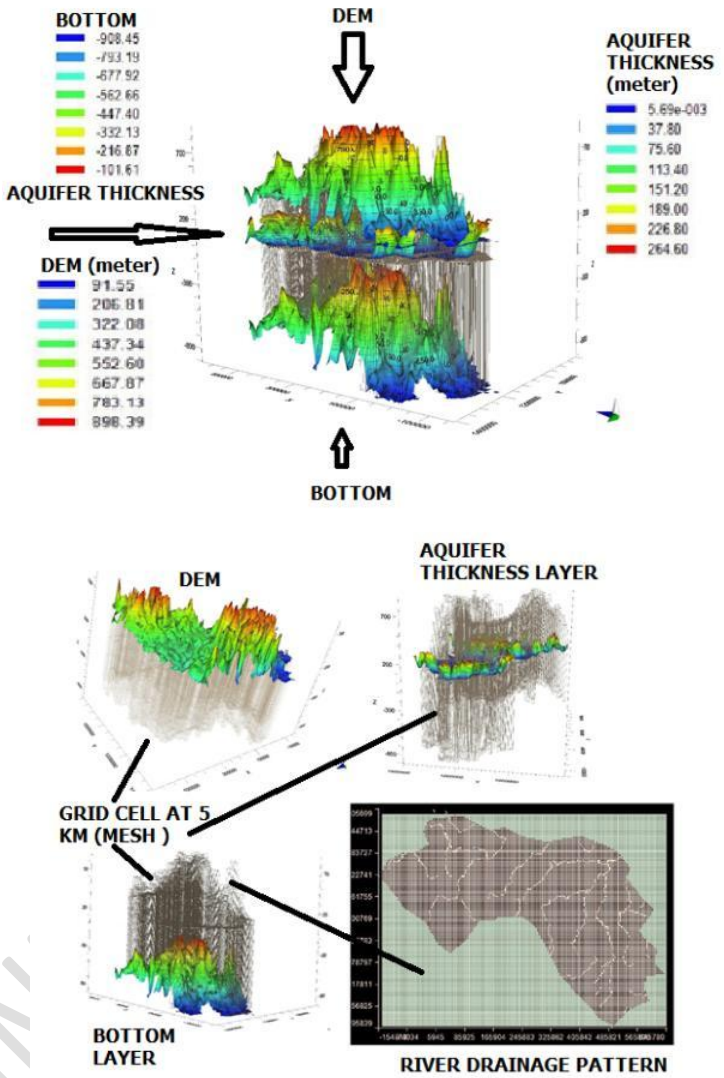

Figure 6 (a) Conceptualt 3D model of Modflow simulation of the Guinea (West Africa) region

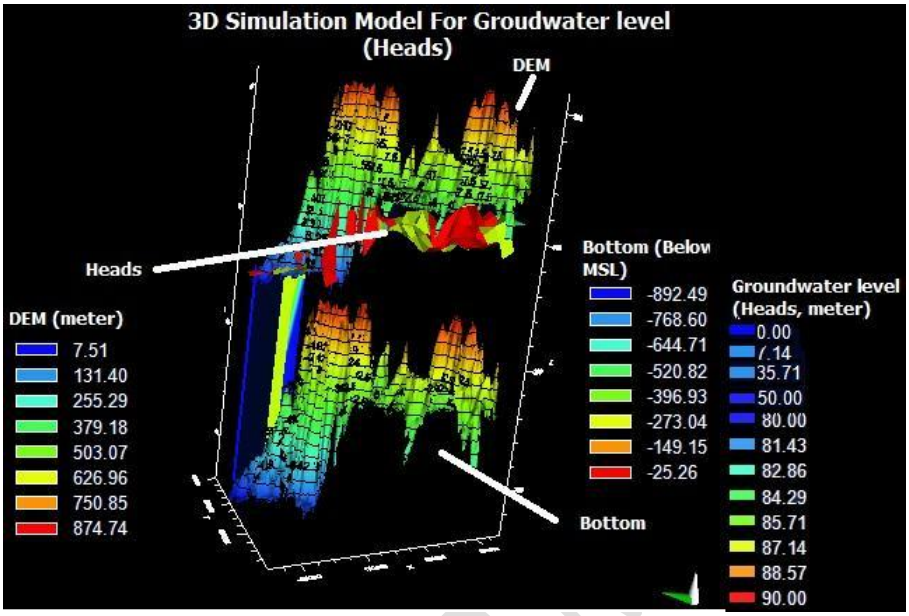

Figure 6 (b) Numerical 3D model of Modflow simulation of the Groundwater levels (Heads) Guinea (West Africa) region